How to cite: *Angew. Chem. Int. Ed.* **2024**, *63*, e202406094
doi.org/10.1002/anie.202406094

Protocells **Hot Paper**

Acyl Phosphates as Chemically Fueled Building Blocks for Self-Sustaining Protocells

*Oleksii Zozulia, Christine M. E. Kriebisch, Brigitte A. K. Kriebisch, Héctor Soria-Carrera, Kingu Rici Ryadi, Juliana Steck, and Job Boekhoven**

Abstract: Lipids spontaneously assemble into vesicle-forming membranes. Such vesicles serve as compartments for even the simplest living systems. Vesicles have been extensively studied for constructing synthetic cells or as models for protocells—the cells hypothesized to have existed before life. These compartments exist almost always close to equilibrium. Life, however, exists out of equilibrium. In this work, we studied vesicle-based compartments regulated by a non-equilibrium chemical reaction network that converts activating agents. In this way, the compartments require a constant or periodic supply of activating agents to sustain themselves. Specifically, we use activating agents to condense carboxylates and phosphate esters into acyl phosphate-based lipids that form vesicles. These vesicles can only be sustained when condensing agents are present; without them, they decay. We demonstrate that the chemical reaction network can operate on prebiotic activating agents, opening the door to prebiotically plausible, self-sustainable protocells that compete for resources. In future work, such protocells should be endowed with a genotype, e.g., self-replicating RNA structures, to alter the protocell's behavior. Such protocells could enable Darwinian evolution in a prebiotically plausible chemical system.

Introduction

Compartmentalization is critical for extant life as it protects biochemical reaction networks, prevents dilution, and the invasion of parasites. In even the simplest forms of life, compartmentalization is achieved through phospholipids that spontaneously assemble into vesicles. Phospholipid-based vesicles have been studied extensively as a model for the cell membrane or as the building blocks for synthetic cells.[1] Moreover, lipids are used as a protocell model for how life could have originated in a compartment-first hypothesis.[2] Excitingly, even simple, prebiotically relevant lipids, like fatty acids, also spontaneously assemble into vesicles. Moreover, such vesicles can grow and spontaneously divide when supplied with building blocks.[3] While fatty acids can assemble into compartments and show exciting life-like behavior, there is a critical difference between such systems and life as we know it. Life maintains itself outside of equilibrium by converting chemical energy and light into the building blocks needed for growth, division, and homeostasis. Even in homeostasis, a cell sustains itself by using resources to regulate its internal chemical reaction networks. For example, the cell continuously remodels existing phospholipids through the Land's cycle.[4] Thus, in an approach towards the *de novo* synthesis of life or to create models for compartments at the origin of life, self-sustainment outside of equilibrium should be considered. In this context, we propose that the compartment can only exist out of equilibrium, whereas in equilibrium, it would dissolve. That way, there is a selection pressure for the compartment to sustain itself away from equilibrium. If not, it would lose its contents, which, in future work, could be genetic material. To do so, we and others coupled the formation of compartments to non-equilibrium chemical reaction cycles.[5] In such a reaction cycle, a molecule with high chemical potential (that we refer to as fuel) is converted into a molecule with low chemical potential (that we refer to as waste).[6] The energy harvested from the fuel-to-waste conversion is used to transiently activate building blocks for compartmentalization. Reaction cycles that convert methylating agents,[7] condensing agents,[8] acylating agents,[9] phosphorylating agents,[10f] and reducing or oxidizing agents[10c–d,11] have been well-explored. The fuel conversion transiently activates a molecule to assemble or phase-separate into a compartment. The activated state is shortlived and spontaneously reverts to its original non-activated state. Thus, at the expense of fuel, molecules are transiently activated to form dynamic, non-equilibrium compartments. The resulting compartments can, therefore, only nucleate when chemical energy is available. These compartments can grow or even divide when energy is abundant.[12] Finally, when all energy is consumed, the compartments decay into their original building blocks. Such self-sustaining compartments constantly compete for resources, making them an attractive model for protocells—protocells that do not produce new building blocks faster

[*] O. Zozulia, C. M. E. Kriebisch, B. A. K. Kriebisch, H. Soria-Carrera, K. R. Ryadi, J. Steck, J. Boekhoven
Department of Bioscience
School of Natural Sciences, Technical University of Munich
Lichtenbergstrasse 4, 85748 Garching, Germany
E-mail: job.boekhoven@tum.de

than their deactivation will naturally succumb, rendering their building blocks available for the competition. We envision small advantages to individual protocells that could be encoded in the protocell's pre-genotype, like self-replicating molecules such as RNA within the protocells that aid the growth or even division of the protocells by catalyzing building block activation. When energy is scarce or only periodically fed to the protocells, those with a genotype that favors growth outcompete those without. While some self-sustaining compartments have been described with exciting behavior like growth[13] and even division,[14] the number of examples that form vesicle-based compartments remains limited.[10a–e] Moreover, examples that produce self-sustaining compartments based on prebiotically plausible chemistry are scarce.[15]

In this work, we developed a self-sustaining chemical system that produces non-equilibrium, transient vesicles based on simple, prebiotically plausible building blocks coupled with acyl phosphate chemistry (Scheme 1). Specifically, we used fatty acids combined with alkyl phosphates as building blocks. When supplied with carbodiimides or prebiotically plausible activating agents, a reaction cycle operates and produces acyl phosphates as an activated product. That product is labile and hydrolyzes to its precursors. However, in its activated state, despite its short lifetime, it can assemble to form dynamic vesicles. These vesicles emerge in response to activating agents. They grow with time and undergo morphological transitions. They compete for activating agents, and when it is consumed, they dissolve. In future work, we envision combining these non-equilibrium compartments with self-replicating RNA sequences. Moreover, the pathway of the formation of primordial phospholipids and, consequently, the question of how permanent compartmentalization emerges is still debated. We envision our system as a possible pre-in-equilibrium event: acyl phosphate vesicles could be both the accumulation reservoirs and the sources of energy[15] for synthesizing more stable phospholipids.

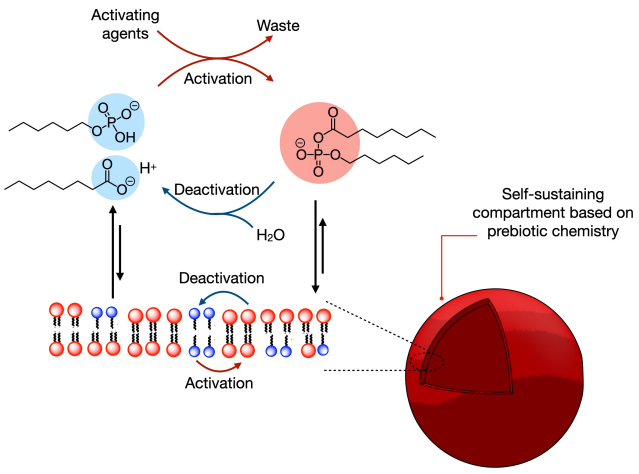

Scheme 1. The chemical reaction cycle based on acyl phosphate chemistry leads to the formation of transient lipids that form out-of-equilibrium compartments.

Results and Discussion

We studied the combination of various carboxylates, alkyl phosphates, and activating agents. As carboxylates, we explored hexanoic (C_6) and octanoic acid (C_8). For the alkyl phosphates, we synthesized hexyl (C_6P) and octyl (C_8P) phosphates as their disodium salts. As activating agents, we used the carbodiimide 1-ethyl-3-(3-dimethyl aminopropyl)carbodiimide (EDC) and condensing agents 2-cyanoguanidine, cyanamide, dicyanamide, and methyl isocyanide. The latter are considered prebiotically plausible, i.e., activating agents that are plausible molecules on early earth as they have been detected in outer space or can easily be synthesized from molecules detected in outer space.[15] We used the activating agents to form the transient acyl phosphates of the acid and alkyl phosphates—a double-tailed amphiphile with an anionic phosphate head group (Figure 1A). All of these components of the reaction cycle were well soluble in the 100 mM range in pyridine-containing 2-morpholinoethanesulfonic acid (MES)-buffered water (200 mM), provided the pH remains above pH 6. Pyridine was added because of its ability to suppress the formation of N-acyl urea and to aid acyl phosphate formation.[16] We performed all experiments at 37 °C and under constant stirring.

Adding 20 mM EDC to a mixture of 40 mM C_6P and 40 mM C_8 initiated the reaction network (Figure 1A). We investigated the kinetic profile of the reaction using high-performance liquid chromatography (HPLC) and confirmed the identity of compounds by mass spectrometry (LCMS) (Figure 1B, Figure S1–3, and Table S2). We observed that the 20 mM EDC was consumed within the first hour after its addition, which resulted in the formation of two new, transient peaks in our chromatogram that were identified to be the acyl phosphate (C_8C_6P) and the symmetric acid anhydride of C_8 (C_8C_8, see Figure S1). The C_8C_8 was short-lived and fully decayed in 2.5 hours. Instead, the C_8C_6P decayed over four days. All EDC was consumed in a short time window while C_8C_8 was still present. In that time, the concentration of C_8C_6P increased, from which we conclude that some of the C_8C_6P was synthesized through the C_8C_8 intermediate (black arrow in Figure 1A), in line with very recent work by von Delius and co-workers.[17] Additionally, we observed a decrease in the concentration for both C_8C_8 and C_8C_6P. We detected up to 100 μM of the by-product N-acylisourea (Figure S4). We further confirmed the absence of detectable amounts of by-products that could be produced by EDC and alkyl phosphates, e.g., dialkyl pyrophosphate.[17] We used the HPLC data to write a kinetic model that predicts the concentration of all species involved in the chemical reaction cycle (See the Supporting Information). The model solves a set of ordinary differential equations and fits it to the experimental data, minimizing an error function using a least mean square method. We validated the kinetic constants we obtained from fitting one set of typical reaction conditions by predicting the kinetic profiles of all compounds involved at different fuel levels and starting acid and phosphate concentrations. The set of rate constants reasonably fitted the experimentally meas-

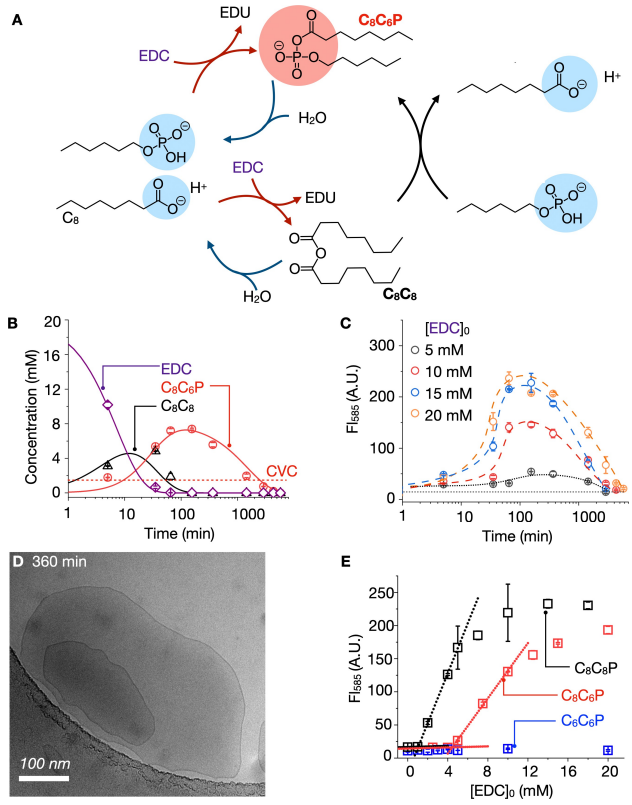

Figure 1. Formation of dynamic, transient acyl phosphate-based vesicles at the expense of activation agents. (A) The acyl phosphate-producing chemical reaction network. (B) The concentrations of the components of the reaction cycle against time when 40 mM C_8 and 40 mM C_6P were fueled with 20 mM EDC at pH 6 in 200 mM MES buffer with 100 mM pyridine. Markers represent the HPLC data, and the solid lines represent data calculated using the kinetic model (sample size $n=3$). (C) MC540 fluorescence intensity against time ($\lambda_{max}=585$ nm) with 5, 10, 15, and 20 mM under otherwise similar conditions as B (sample size $n=3$). The dashed lines are added to guide the eye. (D) A representative cryo-TEM image under the same conditions described in B that was taken after 6 hours. (E) MC540 fluorescence intensity after 4 hours after adding different amounts of fuel. Experiments were performed with C_6 mixed with 40 mM C_6P (blue), 40 mM C_8 mixed with 40 mM C_6P (red), or 20 mM C_8 mixed with 20 mM C_8P (black) in 200 mM MES buffer with 100 mM pyridine (sample size $n=3$).

ured kinetic profiles at varying fuel and starting acid/phosphate concentrations well (Table S1). Using the kinetic model, we calculated the half-life ($t_{1/2}$) of C_8C_6P to be 16 hours.

To study the formation of vesicles, the same reaction (40 mM C_8, 40 mM C_6P, 20 mM EDC) as above was performed in the presence of merocyanine 540 (MC540)—a dye used for quantifying lipid domains.[18] We found that the intensity of the MC540 increased drastically in the first tens of minutes after adding fuel to the reaction solution (Figure 1C). It peaked after two and a half hours (in line with the acyl phosphate formation), steadily declining and reaching its original value after over two days. Adding less fuel, e.g., 15, 10, or 5 mM, shortened the reaction cycle and the maximum emission intensity of the dye. To ensure that the increased intensity originated from forming vesicles, we performed cryogenic transmission electron microscopy (cryo-TEM) imaging of the reaction mixture (Figure 1D). Excitingly, after 6 hours, we found multilamellar vesicles of irregular shape and polydisperse in size. We note that by cryo-TEM, there is a bias towards objects smaller than a few 100 nm. Therefore, we further studied the vesicles by confocal microscopy, which was performed at several time points (Figure S5) in line with the acyl phosphate generation profile. Next, we tested the critical fuel needed to initiate the vesicle formation. As verified above, we would expect the vesicle presence for hours after initiating the reaction network, so we used the MC540 assay as a proxy for vesicle formation by adding it to the reaction network after 4 hours (Figure 1E). For the reaction mixture with C_6P and C_8, we observed the first evidence of vesicles after adding a minimum of 4.5 mM of fuel. Using the kinetic model, we calculated that the reaction cycle had produced a maximum of 1.7 mM of the acyl phosphate C_8C_6P. We thus considered the critical concentration of vesicle formation (CVC) of C_8C_6P to be 1.7 mM. We performed the same experiment with 20 mM C_8P and 20 mM C_8 and found that a minimum of 1.3 mM EDC was required for the first indication of vesicles corresponding to a CVC for C_8C_8P of 0.4 mM (Figure 1E). Noteworthy, the decrease of the CVC by roughly an order of magnitude follows the two-carbon rule of thumb for solubilities of aliphatic organic compounds, such as alcohols. Finally, when C_6 and C_6P were fueled with a maximum of 20 mM EDC, we could not observe any evidence of vesicle formation (Figure S7).

We further investigated the nature of vesicles by confocal fluorescence microscopy again utilizing MC540 to visualize membranes. We used the reaction mixture of 40 mM C_8 with 40 mM C_6P and 20 mM EDC. We obtained confocal micrographs of the reaction mixture at various time points (Figure 2A, Figure S5). After 30 minutes, we found the first evidence of spherical assemblies that were too tiny to resolve—either oil droplets or vesicles. Given that MC540 is charged and preferentially stains bilayers, we assume they were small vesicles, which also aligns with our finding by cryo-TEM. The next several hours of stirring resulted in a large quantity of highly polydisperse vesicles, reaching the micrometer size (Figure S5). After 6 hours, the number of vesicles and their size increased. We observed large vesicles, multiple micrometers in diameter, and their membranes could easily be resolved, with some bright spots starting to emerge. After 15 hours, as the vesicles and C_8C_6P were decaying, we observed that they underwent a morphological transition, i.e., only a few large vesicles were found, and most had merged with a large, spherical assembly that had incorporated a large amount of MC540, given their high fluorescence intensity. After 24 hours, no vesicles were detected in the reaction mixture; instead, there were just bright micrometer-sized spherical assemblies. To further verify this behavior, we synthesized acyl phosphate C_8C_6P. We added it to the pyridine-buffer mixture that contained C_6P, C_8, and the urea (EDU, a product of EDC hydration), to obtain the final concentrations of 8 mM C_8C_6P, 20 mM EDU, and 32 mM of each starting material. Subsequent

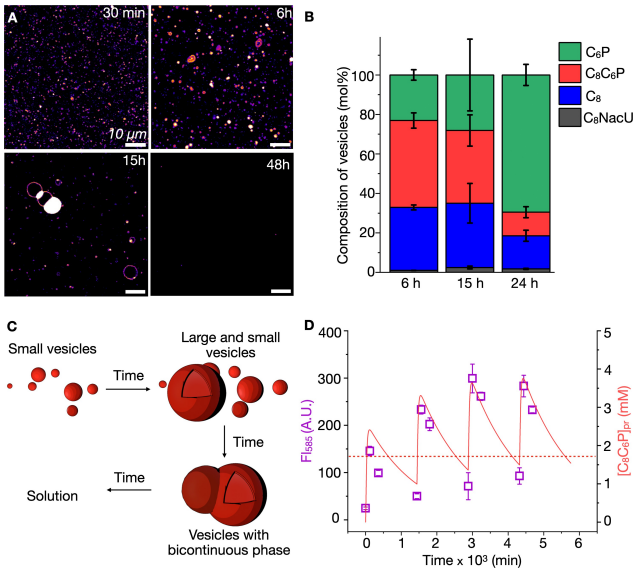

Figure 2. (A) Confocal micrographs of 40 mM C_8 and 40 mM C_6P fueled with 20 mM EDC in 200 mM MES buffer and 100 mM pyridine. Various time points demonstrate the formation of the vesicles and their transition to the bicontinuous phase in the later stages of the reaction cycle with subsequent decay. (B) The composition of the vesicles at various time points of the reaction cycle (sample size $n=3$). (C) Schematic representation of the emergence and morphological transition of the vesicles during the reaction cycle. (D) The evolution of the MC540 fluorescence intensity (violet squares) under the conditions as in A except for multiple refueling steps after each 24-hour cycle. In successive batches, we added 6 mM, 5 mM, and twice 3.8 mM EDC. The red solid line (corresponding to the right y-axis) represents the concentration of $[C_8C_6P]_{pr}$ predicted by the kinetic model. For clarity, the red dashed line represents the CVC_{C8C6P} (sample size $n=3$).

confocal microscopy (Figure S8) revealed the emergence of similar compartment structures and morphological transitions similar to the one described above for the EDC-induced reaction network.

We hypothesize that the spherical assembly is a sponge-like, continuous lipid phase[19] given that it had incorporated more MC540 than in a typical bilayer. Moreover, cryo-TEM after 24 hours revealed the formation of a sponge-like phase with interlamellar attachment points (Figure S9). After 48 hours, the sample was mostly free of any assemblies corroborating the transient nature of the vesicles. To investigate the nature of the compartments further, we isolated them from their surrounding solution by spinning them down in a centrifuge after 6, 15, and 24 hours. The pellet was resuspended in buffer and analyzed by HPLC and ^{31}P-qNMR for its composition (Figure 2B). Early in the cycle, i.e., after 6 or 15 hours, the vesicles comprised almost equal parts of the C_6P, C_8, and C_8C_6P. Later in the cycle, we found that the fraction of C_6P had increased at the cost of both C_8 and C_8C_6P. Noteworthy is that the reaction cycle with C_8 and C_8P also produced vesicles, as evidenced by confocal and electron microscopy (Figure S6 and S10).

From the data above, we established a tentative model to describe the self-assembly process of the components in the reaction cycle in response to chemical fuel (Figure 2C). First, the self-assembly can only occur in response to fuel, from which we conclude that the formation of the acyl phosphate C_8C_6P drives the bilayer formation. Nevertheless, the assembly is a co-assembly of C_6P, C_8, and C_8C_6P, as evidenced by the spin-down experiments. We hypothesize that all components co-assemble to form a bilayer with the aliphatic tails pointing inward. As the system runs out of chemical fuel, no new C_8C_6P is formed. Thus, with time, the C_8C_6P concentration decreases, which also changes the ratio of the components in the assembly—more C_6P and C_8 get accumulated in the structures. That shift in the ratio drives a change in the packing of the bilayer, such that a bicontinuous bilayer phase is formed comprised mostly of C_6P. Finally, when all C_8C_6P is hydrolyzed, the bicontinuous bilayer phase dissolves, and the system is reset.

Importantly, we verified the reaction cycle, and consequently, the assembly process can be reinitiated several times by adding new portions of the fuel (Figure 2D). For this, we started the reaction network (40 mM C_8, 40 mM C_6P) by adding only 6 mM EDC, roughly 34 % more than required to produce C_8C_6P enough to reach the CVC. After 2 hours, we investigated the reaction mixture using MC540 assay and observed a fluorescence enhancement indicative of the presence of bilayers. This reaction was left for 24 hours under constant stirring at 37 °C and the new MC540 tests revealed the substantial decay of the fluorescence. Subsequent refueling of the same reaction mixture with the smaller portions of EDC (5 mM, then 3.8 mM, and 3.8 mM) within the next days led to the same 24-hour fluorescence enhancement/decay cycle, albeit with intensities higher than in the initial 24-hour cycle. This fact can be explained by utilizing the kinetic model (red trace and right y-axis in Figure 2D) which predicts for our refueling regime the residual accumulation of $[C_8C_6P]_{pr}$ after each 24-hour cycle to be very close to the CVC (see the dashed line in Figure 2D), thus causing the fluorescence intensity to be always above the non-initiated point (0-minute, before EDC addition) as well as higher than the signal intensity after the first refueling. Noteworthy, after the last refueling step, the fluorescence intensity approached the starting value after 2.5 days (Figure S13). In brief, with that refueling regime, we demonstrated that assembly into bilayers can be repeated multiple times as it correlates with the evolution of the acyl phosphate concentration above or within the CVC.

Next, we tested whether the self-sustaining vesicles from simple building blocks could also be formed using prebiotically plausible fuels. Instead of EDC, we thus used the condensing agents 2-cyanoguanidine, cyanamide, dicyanamide, and methyl isocyanide (Figure 3A), all of which have been proposed to be present on early Earth before the emergence of life.[20] We used 100 mM of each condensing agent to fuel the reaction networks of 40 mM of C_8 and C_6P. Unlike the previous experiments, we did not use MES as a buffer to make the self-sustaining vesicles more prebiotically plausible, but we kept using pyridine as a catalytic component. Prebiotically relevant alternatives for pyridine have been proposed in the literature.[21] For 2-cyanoguanidine and cyanamide, we found no evidence of the acyl phosphate even by LCMS. We found only traces of the acyl

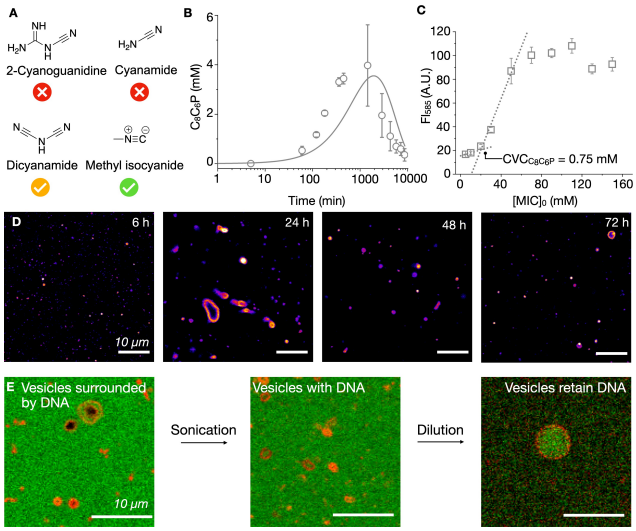

Figure 3. Self-sustaining vesicles by prebiotic fuels. (A) Different prebiotically relevant fuels were tested in the acyl phosphate-producing reaction cycle. (B) The concentration of C_8C_6P against time when 40 mM C_8 and 40 mM C_6P were fueled with 100 mM methylisocyanide (sample size $n=3$). The solid line represents the data predicted by a kinetic model. (C) The MC540 fluorescence intensity was measured 24 hours after adding different amounts of methyl isocyanide to a solution as described in B (sample size $n=3$). (D) Confocal micrograph of the solution described in B at various time points. (E) Confocal micrographs of the vesicle solution in the presence of the fluorescently labeled DNA.

phosphate for dicyanamide in the mass spectrometer (Figure S14). We speculate that the activation is inefficient in the case of these fuels, probably because they require a much more acidic environment to tautomerize into active forms (e.g., cyanamide to carbodiimide) efficiently. Excitingly and in line with the elevated reactivity of methyl isocyanide,[20d,22] we observed up to 4 mM of the acyl phosphate C_8C_6P. Like the experiments above, we followed the evolution of the reaction cycle by HPLC and confirmed the emergence and decay of C_8C_6P by LCMS. (Figure 3B and Figures S11 and S12). The methyl isocyanide consumption was determined by ^{1}H NMR spectroscopy (Figure S15). The concentration of C_8C_6P increased and peaked at around 24 hours, i.e., later than in the case when we used EDC as fuel (after 2.5 hours). After that, the C_8C_6P concentration decayed steadily over the next few days. We refitted the HPLC data using the kinetic model, which verified that the activation was slower with methyl isocyanide as fuel than with EDC. Importantly, we confirmed that the pH did not change throughout the experiment despite lacking a buffer (Table S3). Next, we used the MC540 assay to verify that the system could produce self-sustaining vesicles using methyl isocyanide as a fuel. We measured the intensity of the MC540 emission 24 hours after adding different amounts of fuel and determined that a minimum of 20 mM of methyl isocyanide was needed to induce vesicle formation (Figure 3C). Using the kinetic model, we calculated that this corresponded to a critical vesicle concentration of 0.75 mM C_8C_6P, which aligns with the CVC found for EDC as fuel.

We imaged the solutions formed with 100 mM methyl isocyanide using confocal microscopy (Figure 3D and Figure S12). In line with using EDC as fuel, we found the emergence of small vesicles, which grew into large vesicles. Again, towards the end of the cycle, the vesicles transitioned into vesicles with a bicontinuous phase.

Finally, we probed the permeability of the membranes of the methyl isocyanide-driven, acyl phosphate-based vesicles to demonstrate that they can serve as a compartment for a self-replicating information carrier in future work (Figure 3E, Figure S16). We initiated the reaction network with methyl isocyanide as described above. After 24 hours, we added fluorescently labeled DNA and MC540. Confocal microscopy demonstrated that most of these vesicles had not taken up any DNA. In other words, the membrane bilayer is a barrier to prevent the spontaneous invasion of polyanions. We sonicated the solution briefly and found that most vesicles now contained DNA at roughly equal intensity outside and inside. When we diluted the vesicle solutions with a separately prepared reaction mixture without DNA, we found the vesicles had a higher concentration of DNA inside the vesicle than outside (Figure 3E, Figure S16). Thus, the vesicles form a barrier to protect their contents from polyanions from the outside while retaining them inside.

Conclusion

We presented an acyl phosphate chemical reaction network that produces self-sustaining, dynamic vesicles based on simple molecules and driven by the conversion of activating agents. The reagents used in the network have been demonstrated to be prebiotically plausible, and the fuel-dependent vesicles could thus be used as a protocell model. A challenge of these systems is the accumulation of waste that could hinder further growth. In future work, we will combine these self-sustaining vesicles with catalysts and RNA sequences to test whether a pre-genotype, in the form of information-containing RNA, can influence the behavior of the protocells, for example, their ability to survive starvation periods or their ability to divide.

Supporting Information

The authors have cited additional references within the Supporting Information.[23]

Acknowledgements

The BoekhovenLab is grateful for support from the TUM Innovation Network - RISE funded through the Excellence Strategy and the European Research Council (ERC starting grant 852187). This research was conducted within the Max Planck School Matter to Life, supported by the German Federal Ministry of Education and Research (BMBF) in collaboration with the Max Planck Society. This research

was supported by the Excellence Cluster ORIGINS, which is funded by the Deutsche Forschungsgemeinschaft (DFG, German Research Foundation) under Germany's Excellence Strategy—EXC-2094-390783311. H.S.-C thanks the Alexander von Humboldt Foundation for a postdoctoral research

fellowship. Cryo-TEM measurements were performed using infrastructure contributed by the Dietz Lab and the TUM EM Core Facility. We acknowledge the technical support provided by Fabian Kohler and are grateful to Dr. Pablo Zambrano for valuable discussions. Open Access funding enabled and organized by Projekt DEAL.

Conflict of Interest

The authors declare no conflict of interest.

Data Availability Statement

The data that support the findings of this study are available from the corresponding author upon reasonable request.

Keywords: chemically fueled self-assembly · self-sustaining compartments · protocells · acyl phosphate

[1] a) X. Wang, H. Du, Z. Wang, W. Mu, X. Han, *Adv. Mater.* **2021**, *33*, 2002635; b) Y. Lu, G. Allegri, J. Huskens, *Mater. Horiz.* **2022**, *9*, 892–907.

[2] a) M. M. Hanczyc, S. M. Fujikawa, J. W. Szostak, *Science* **2003**, *302*, 618–622; b) I. A. Chen, R. W. Roberts, J. W. Szostak, *Science* **2004**, *305*, 1474–1476.

[3] a) T. F. Zhu, J. W. Szostak, *J. Am. Chem. Soc.* **2009**, *131*, 5705–5713; b) C. Hentrich, J. W. Szostak, *Langmuir* **2014**, *30*, 14916–14925; c) M. M. Hanczyc, J. W. Szostak, *Curr. Opin. Chem. Biol.* **2004**, *8*, 660–664; d) Z. R. Todd, Z. R. Cohen, D. C. Catling, S. L. Keller, R. A. Black, *Langmuir* **2022**, *38*, 15106–15112.

[4] B. Wang, P. Tontonoz, *Annu. Rev. Psychol.* **2019**, *81*, 165–188.

[5] a) C. Donau, F. Späth, M. Stasi, A. M. Bergmann, J. Boekhoven, *Angew. Chem. Int. Ed.* **2022**, *61*, e202211905; b) C. Wanzke, A. Jussupow, F. Kohler, H. Dietz, V. R. I. Kaila, J. Boekhoven, *ChemSystemsChem* **2020**, *2*, e1900044.

[6] a) X. Chen, M. A. Würbser, J. Boekhoven, *Acc. Mater. Res.* **2023**, *4*, 416–426; b) P. S. Schwarz, M. Tena-Solsona, K. Dai, J. Boekhoven, *Chem. Commun.* **2022**, *58*, 1284–1297; c) B. Rieß, R. K. Grötsch, J. Boekhoven, *Chem* **2020**, *6*, 552–578.

[7] a) J. Boekhoven, W. E. Hendriksen, G. J. M. Koper, R. Eelkema, J. H. van Esch, *Science* **2015**, *349*, 1075–1079; b) B. G. P. van Ravensteijn, W. E. Hendriksen, R. Eelkema, J. H. van Esch, W. K. Kegel, *J. Am. Chem. Soc.* **2017**, *139*, 9763–9766.

[8] a) L. S. Kariyawasam, C. S. Hartley, *J. Am. Chem. Soc.* **2017**, *139*, 11949–11955; b) M. M. Hossain, J. L. Atkinson, C. S. Hartley, *Angew. Chem. Int. Ed.* **2020**, *59*, 13807–13813; c) M. Tena-Solsona, B. Rieß, R. K. Grötsch, F. C. Löhrer, C. Wanzke, B. Käsdorf, A. R. Bausch, P. Müller-Buschbaum, O. Lieleg, J. Boekhoven, *Nat. Commun.* **2017**, *8*, 15895; d) M. Tena-Solsona, C. Wanzke, B. Riess, A. R. Bausch, J. Boekhoven, *Nat. Commun.* **2018**, *9*, 2044; e) S. Borsley, E. Kreidt, D. A. Leigh, B. M. W. Roberts, *Nature* **2022**, *604*, 80–85; f) S. P. Afrose, S. Bal, A. Chatterjee, K. Das, D. Das, *Angew. Chem. Int. Ed.* **2019**, *58*, 15783.

[9] M. P. van der Helm, C.-L. Wang, B. Fan, M. Macchione, E. Mendes, R. Eelkema, *Angew. Chem. Int. Ed.* **2020**, *59*, 20604–20611.

[10] a) S. Maiti, I. Fortunati, C. Ferrante, P. Scrimin, L. J. Prins, *Nat. Chem.* **2016**, *8*, 725–731; b) H. H. Zepik, E. Blöchliger, P. L. Luisi, *Angew. Chem. Int. Ed.* **2001**, *40*, 199–202; c) A. H. J. Engwerda, J. Southworth, M. A. Lebedeva, R. J. H. Scanes, P. Kukura, S. P. Fletcher, *Angew. Chem. Int. Ed.* **2020**, *59*, 20361–20366; d) S. M. Morrow, I. Colomer, S. P. Fletcher, *Nat. Commun.* **2019**, *10*, 1–9; e) E. A. J. Post, S. P. Fletcher, *Chem. Sci.* **2020**, *11*, 9434–9442; f) A. Sorrenti, J. Leira-Iglesias, A. Sato, T. M. Hermans, *Nat. Commun.* **2017**, *8*, 15899.

[11] a) C. Chen, J. S. Valera, T. B. M. Adachi, T. M. Hermans, *Chem. Eur. J.* **2023**, *29*, e202202849; b) A. Sharko, B. Spitzbarth, T. M. Hermans, R. Eelkema, *J. Am. Chem. Soc.* **2023**, *145*, 9672–9678; c) E. Del Grosso, L. J. Prins, F. Ricci, *Angew. Chem. Int. Ed.* **2020**, *59*, 13238–13245.

[12] D. Zwicker, R. Seyboldt, C. A. Weber, A. A. Hyman, F. Jülicher, *Nat. Phys.* **2017**, *13*, 408–413.

[13] K. K. Nakashima, M. H. I. van Haren, A. A. M. André, I. Robu, E. Spruijt, *Nat. Commun.* **2021**, *12*, 3819.

[14] C. Donau, F. Späth, M. Sosson, B. A. Kriebisch, F. Schnitter, M. Tena-Solsona, H.-S. Kang, E. Salibi, M. Sattler, H. Mutschler, *Nat. Commun.* **2020**, *11*, 1–10.

[15] C. Bonfio, C. c Caumes, C. D. Duffy, B. H. Patel, C. Percivalle, M. Tsanakopoulou, J. D. Sutherland, *J. Am. Chem. Soc.* **2019**, *141*, 3934–3939.

[16] a) X. Chen, H. Soria-Carrera, O. Zozulia, J. Boekhoven, *Chem. Sci.* **2023**, *14*, 12653–12660; b) X. Chen, M. Stasi, J. Rodon-Fores, P. F. Großmann, A. M. Bergmann, K. Dai, M. Tena-Solsona, B. Rieger, J. Boekhoven, *J. Am. Chem. Soc.* **2023**, *145*, 6880–6887.

[17] A. Englert, F. Majer, J. L. Schiessl, A. J. C. Kuehne, M. von Delius, *Chem* **2024**, *10*, 910–923.

[18] a) P. Williamson, K. Mattocks, R. A. Schlegel, *Biochim. Biophys. Acta Biomembr.* **1983**, *732*, 387–393; b) M. Langner, S. W. Hui, *Biochim. Biophys. Acta Biomembr.* **1999**, *1415*, 323–330; c) C. Watala, I. Waczulikova, B. Wieclawska, M. Rozalski, P. Gresner, K. Gwoździński, A. Mateasik, L. Šikurova, *Cytometry* **2002**, *49*, 119–133; d) R. Dutta, A. Pyne, S. Kundu, P. Banerjee, N. Sarkar, *Langmuir* **2017**, *33*, 9811–9821.

[19] A. P. Schroder, J. J. Crassous, C. M. Marques, U. Olsson, *Sci. Rep.* **2019**, *9*, 2292.

[20] a) C. M. Nichols, Z.-C. Wang, Z. Yang, W. C. Lineberger, V. M. Bierbaum, *J. Phys. Chem. A* **2016**, *120*, 992–999; b) A. J. Remijan, J. M. Hollis, F. J. Lovas, D. F. Plusquellic, P. Jewell, *Astrophys. J.* **2005**, *632*, 333; c) A. Mariani, D. A. Russell, T. Javelle, J. D. Sutherland, *J. Am. Chem. Soc.* **2018**, *140*, 8657–8661; d) Z. Liu, L.-F. Wu, J. Xu, C. Bonfio, D. A. Russell, J. D. Sutherland, *Nat. Chem.* **2020**, *12*, 1023–1028.

[21] Z. Liu, L.-F. Wu, J. Xu, C. Bonfio, D. A. Russell, J. D. Sutherland, *Nat. Chem.* **2020**, *12*, 1023–1028.

[22] S. J. Zhang, D. Duzdevich, J. W. Szostak, *J. Am. Chem. Soc.* **2020**, *142*, 14810–14813.

[23] S. L. Morales-Lázaro, B. Serrano-Flores, I. Llorente, E. Hernández-García, R. González-Ramírez, S. Banerjee, D. Miller, V. Gududuru, J. Fells, D. Norman, *J. Biol. Chem.* **2014**, *289*, 24079–24090.

Manuscript received: March 29, 2024
Accepted manuscript online: May 14, 2024
Version of record online: June 19, 2024